Geoscience Letters

RESEARCH LETTER

Open Access

A fresh look at the intensity and impulsive strength of geomagnetic storms

V. Manu[1,2], N. Balan[1], Y. Ebihara[3], Qing-He Zhang[1*] and Zan-Yang Xing[1]

Abstract

We notice that the important early decreasing part of the main phase (MP) from the positive main phase onset (MPO) to 0-level of Dst and SymH indices is missed in the treatment of the main phase (MP) of geomagnetic storms. We correct this inconsistency in 848 storms having positive MPO (out of 1164 storms) in SymH during 1981–2019 by raising the 0-level of SymH to the MPO-level. The correction considers the full range of the main phase, increases the corrected (revised) storm intensity (SymHMin*) and impulsive strength (IpsSymH*) by up to − 149 nT and − 134 nT, respectively, and seems important for all aspects of global space weather. For example, the corrected SymHMin* changes the conventional storm identification and classification and corrected IpsSymH* clearly identifies all 3 severe space weather (SvSW) events from over 1100 normal space weather (NSW) events with a separation of 52 nT; it also identifies all 8 minor-system-damage space weather (MSW) events from the NSW events.

Key points

- We correct an inconsistency in the SymH values during the MP and RP of the 848 storms having positive MPO during 1981–2019.
- The corrected values of SymHMin* and IpsSymH* increase by up to − 149 nT and − 134 nT compared to their uncorrected values.
- The correction changes the storm identification and clearly identifies all 3 SvSW and 8 MSW events from over 1100 NSW events.

Keywords Geomagnetic storms, Positive MPO, Storm intensity and impulsive strength

Plain Language Summary

Large fluctuations occur in the global geomagnetic field during space weather events. The fluctuations at low latitudes are referred as geomagnetic storms. The Dst and SymH indices have been used for studying the storms and other aspects of global space weather. However, we notice that the Dst and SymH values during the main phase and recovery phase of the storms having positive main phase onset (MPO > 0 nT) are significantly less than their actual values. We correct this inconsistency in 848 such storms (out of 1164 storms) in SymH during 1981-2019 by raising the 0-level of SymH to the MPO-level. The corrected/revised storm intensity (SymHMin*) and impulsive strength (IpsSymH*) increase by up to − 149 and − 134 nT. The correction seems important for studying all aspects global space

*Correspondence:
Qing-He Zhang
zhangqinghe@sdu.edu.cn
Full list of author information is available at the end of the article

weather. For example, the correction identifies the storms corresponding to severe space weather causing power outage and/or telecommunication failure from those corresponding to normal space weather.

Introduction

The large electric currents flowing at different regions in the magnetosphere and ionosphere during space weather events produce large fluctuations in the geomagnetic field lasting up to several days in all latitudes (e.g., Chapman and Bartels 1940). The field fluctuations at low latitudes are referred as geomagnetic storms. The storms have been studied using the Dst index (Sugiura 1964; Love and Cannon 2009) and SymH index (Iyemori et al. 1992). Sugiura (1964) developed the Dst index of 1-h resolution from the H-component magnetic field measured at 4 low latitude observatories (3 in north and 1 in south) outside the influence of the equatorial electrojet and having maximum longitude separation (MLS) of ~120°. To improve the time and spatial resolutions, the SymH index of 1-min resolution was developed (Iyemori et al. 1992) using the H-component data from up to 6 stations of MLS ~70°. The Dst and SymH indices have been used for studying not only the geomagnetic storms (e.g., Russell et al. 1973; Burton et al. 1975a; Ebihara et al. 2003, 2005; Gonzalez et al. 2011; Gopalswamy et al. 2015; Yermolaev et al. 2021; Balan et al. 2021; Manu et al. 2022, 2023) but also the disturbed upper atmosphere, ionosphere and magnetosphere (e.g., Fuller-Rowell et al. 1994; Manuucci et al. 2005; Tulasiram et al. 2010; Balan et al. 2013). For reviews, see Akasofu (1981, 2021), Proless (1995), Daglis (1997), Luhr et al. (2017) and Zong et al. (2021).

The geomagnetic storms (Fig. 1) are characterized by 3-phases—the initial phase (IP), main phase (MP) and recovery phase (RP) (Russell et al. 1974; Burton et al. 1975b; Gonzalez et al. 1994; Araki et al. 1997; Hutchinson et al. 2011). The initial phase (IP), however, may not be visible in the case of the storms starting from significant negative value of the indices. The positive initial phase (IP) is considered to be caused by the combined effect of the sudden compression of the magnetosphere at the impulsive impact of the interplanetary coronal mass ejection (ICME) front of suddenly enhanced solar wind dynamic pressure P and IMF Bz northward (Burton et al. 1975b; Shue et al. 1998; Balan et al. 2008; Wang et al. 2018) and eastward magnetopause current induced by the enhanced P when IMF Bz remains northward (e.g.,Araki et al. 1997, 2014). The main phase starts at MPO (main phase onset) when pressure P decreases and IMF Bz turns southward (Burton et al. 1975a,b; Gonzalez et al. 1994; Hutchinson et al. 2011). During the main phase (MP) when IMF Bz remains southward, SymH continues to decrease due to the increase in westward ring current and other minor currents such as tail current, field aligned current, etc. As the currents causing the MP build up, their decay also increases. When the currents' growth rate balances the decay rate, the MP reaches its peak or SymH reaches its maximum negative value (SymHMin), which is considered as the storm intensity (e.g., Burton et al. 1975b; Gonzalez et al. 1994; Hutchinson et al. 2011). The storm recovers back to the quiet-time level taking up to several days. Conventionally, the storms are classified as minor ($-25 \geq$ SymHMin > -50 nT), moderate ($-50 \geq$ SymHMin > -100 nT), intense ($-100 \geq$ SymHMin > -250 nT) and super (SymHMin ≤ -250 nT).

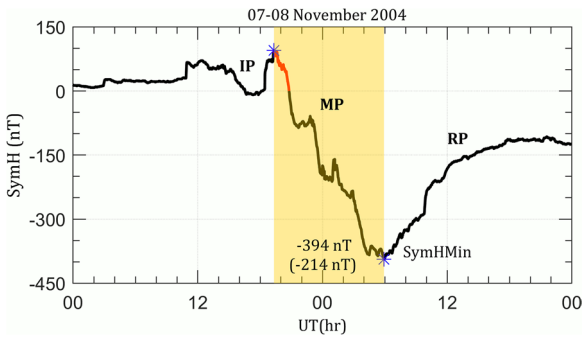

Fig. 1 A geomagnetic storm having positive main phase onset (MPO). The missed early part of the main phase (MP) is highlighted in red

The storm impulsive strength IpsDst was defined (Balan et al. 2016, 2019a) as

$$IpsDst = -\frac{1}{T_{MP}} \int |Dst| dt \quad (1)$$

where $\int |Dst| dt$ is the sum of the modulus of Dst from MPO to DstMin and T_{MP} is the MP duration (in hours) from MPO to DstMin which is numerically equal to N-1 with N being the number of data points both ends inclusive. By definition, IpsDst gives the negative of the modulus of mean Dst from MPO to DstMin. Physically, the numerator $\int |Dst| dt$ is proportional to the solar wind energy input into the ring current (and magnetosphere) (Burton et al. 1975a, b) and denominator T_{MP} is the duration of the energy input. Higher the energy input and shorter the duration, the larger the IpsDst. In other words, IpsDst physically represents the impulsive action of space weather events and therefore the name *impulsive Dst* (or *IpsDst*) (Balan et al. 2019a, b).

However, the IpsDst given by Eq. (1) is not appropriate for comparison after correcting for the missed decreasing part of positive MPO (subject of this paper) because Eq. (1) partially includes the correction from MPO to original 0-level of Dst in $\int |Dst|dt$. Therefore, here we define the IpsSymH having no correction for comparison with the IpsSymH having full correction (IpsSymH*, section "Correction and physical meaning") in SymH index as

$$IpsSymH = \frac{1}{T_{MP}} \int SymHdt \tag{2}$$

where $\int SymHdt$ is the sum of SymH from the original 0-level of SymH to SymHMIn and T_{MP} is the MP duration in minutes from 0-level to SymHMin (Fig. 1).

Though the main phase MP starts from MPO, the early decreasing part of MP from positive MPO to the original 0-level of SymH (and Dst) shown by the highlighted red part in Fig. 1 is, somehow, missed in the treatment of the main phase (MP) in the literature. This missing part of MP makes the SymH (and Dst) values during the MP and RP significantly less than their actual values. In this paper, we correct this inconsistency in the clear storms identified in SymH during 1981–2019. The correction done for the first time significantly increases the storm intensity (SymHMin*) and impulsive strength (IpsSymH*) and therefore seems important for all aspects of global space weather. We discuss the importance for two aspects and mention the importance for two other aspects. The correction is most important for the storm impulsive strength (IpsSymH*), section "Identification of SvSW and MSW events".

Automatic storm identification

The SymH index is available at http://wdc.kugi.kyoto-u.ac.jp/aeasy/index.html. The 4 selection criteria used for identifying the storms in Dst index (Balan et al. 2017a) are modified for identifying the storms in SymH including minor storms (Table 1). First, assuming the largest peak in the initial phase IP (IP-largest) within 8 h prior to SymH turning negative as MPO, the program identifies 1164 clear storms including 848 storms having positive MPO. Since the initial phase IP can have one or more peaks due to fluctuations in the solar wind dynamic pressure P and/or IMF Bz, a new criterion 5 as in Table 1 is used for separating the storms having (715) IP-largest and (133) IP-large as MPO (Fig. 2a, b) where IP-large is the second largest peak in IP after IP-largest. (Criterion 5 is fixed after trying a number of similar options. For higher values of IP-large, the program picks up the small

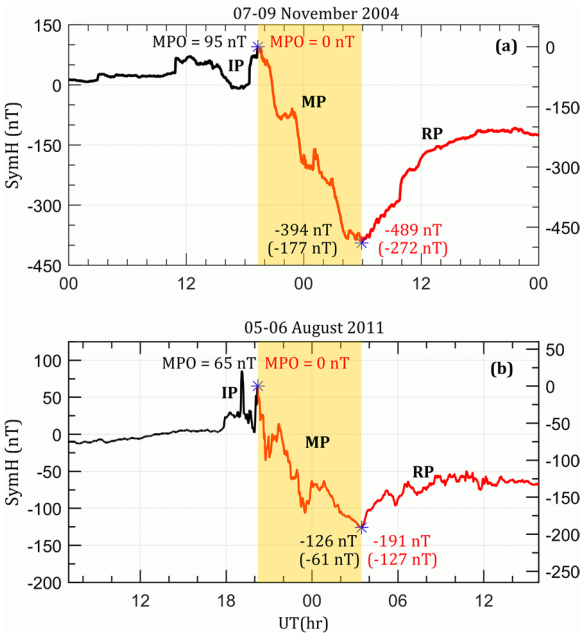

Fig. 2 Examples of the correction for two storms having IP-largest (**a**) and IP-large (**b**) as MPO. The original values (LHS scale) and corrected values (RHS scale) of MPO, SymHMin and IpsSymH (in brackets) are noted

Table 1 Table lists the storm selection criteria1-5, their advantages, total number of storms and those having positive MPO identified by the successive applications of the criteria

Criterion	Advantage	Criteria	No. of storms	No. with + MPO
1. SymHMin ≤ − 25 nT and T_{MP} > 2 h	Avoids short-period negative fluctuations	1	7142	1906
2. $\lvert SymH_{MPO} - SymHMin \rvert \geq 50$ nT	Includes positive MPO	1–2	1563	1109
3. Separation from SymHMin to next MPO ≥ 10 h	Identifies storms due to separate drivers (e.g., ICMEs)	1–3	1446	1081
4. Average $(dSymH/dt)_{MP} < -5$ nT/hr	Avoids non-storm-like long duration negative decreases	1–4	1164	848
5. If IP-large ≥ 60% and minimum ≤ 40% of IP-largest, the IP-large and otherwise IP-largest are used as MPO	Identifies the largest or large peak in IP as MPO	1–5	–	715 (IP-largest) 133 (IP-large)

fluctuations in IP-largest as IP-large and for lower values of the minimum, the number of IP-large becomes very small).

Correction and physical meaning

Since the main phase (MP) starts from the main phase onset MPO when SymH starts decreasing (e.g., Gonzalez et al. 1994; Hutchinson et al. 2011), the 0-level of SymH during MP (and RP) has to be at the MPO-level to account for the full range of MP. In other words, the inconsistency in the storms having positive MPO can be corrected by raising the (original) '0-level' of SymH to the MPO-level as shown in Fig. 2a, b (RHS scale). The corrected storm intensity SymHMin* is the maximum negative value of SymH during the MP (RHS scale) and corrected storm impulsive strength IpsSymH* becomes

$$IpsSymH^* = \frac{1}{T_{MP}{}^*} \int SymHdt \tag{3}$$

where $\int SymHdt$ in Eq. (3) is the sum of SymH from MPO to SymHMin* and $T_{MP}{}^*$ is the corrected MP duration in minutes (Fig. 2, RHS scale). In Eqs. (2) and (3), the negative sign and modulus in the integral got removed compared to Eq. (1). In the examples in Fig. 2a and b, the corrected (or revised) storm intensity SymHMin* increases from −394 nT to −489 nT and from to −126 nT to −191 nT, and the corrected impulsive strength IpsSymH* increases from −214 nT to −272 nT and from to −68 nT to −127 nT. The revised SymHMin* and IpsSymH* of all storms having positive MPO are found to be more negative than their values having no correction (Fig. 3),

which seems to validate the correction procedure. The corrected SymHMin* increases by the largest positive MPO of up to −149 nT and corrected IpsSymH* increases by a slightly smaller amount by up to −134 nT (Fig. 3). The correction can be gradually terminated during RP from the point when the negative SymH becomes equal to the positive MPO to the (original) end of RP. The physical meaning of the correction is briefly discussed in section "Discussion".

Importance of the correction

Here we discuss the importance of the correction for two aspects of global space weather and mention the importance for two other aspects.

Storm identification and classification

As listed in Table 2, originally there are 282 minor storms. But, after correction, only 14 storms remain minor; of the remaining storms, 264 become moderate and 4 become intense. There are 599 moderate storms with no correction. After correction, there are 480 moderate storms and

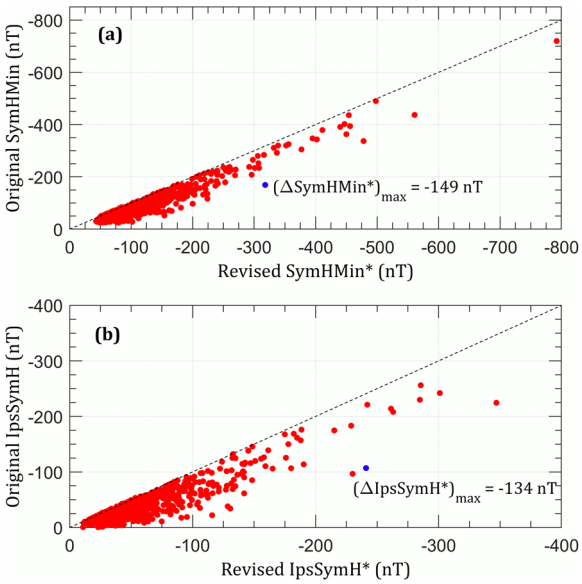

Fig. 3 Original (Y-axes) SymHMin (**a**) and IpsSymH (**b**) against revised (X-axes) SymHMin* and IpsSymH*. The maximum increases (ΔSymHMin)max and (ΔIpsSymH)max are noted

Table 2 Number of minor, moderate, intense and super storms before and after correction

Type of original storms	Number of original storms	Number of storms after correction			
		Minor	Moderate	Intense	Super
Minor	282	14	264	4	–
Moderate	599	–	480	119	–
Intense	256	–	–	241	15
Super	27	–	–	–	27
Total	1164	14	744	364	42

119 intense storms. Of the 256 intense storms before correction, 241 remain intense and 15 become super after correction. Including these 15 and the original 27, there are 42 super storms after correction. As shown in Fig. 4a, d, the intensity of the original minor storms (> −50 nT) increases up to −112 nT, moderate storms (> −100 nT) increase up to −200 nT, intense storms (> −250 nT) increases up to −318 nT, and super storms (≤ −250 nT) increases up to −792 nT. In short, the correction for positive MPO changes the conventional storm identification and classification. In panel (a) for the original minor storms (−25 ≥ SymHMin > −50 nT), there is no blue dot (absence of negative MPO) and SymHMin* starts from a much larger level than expected (−25 nT) and increases up to −112 nT. These facts indicate that all 282 original minor storms have large positive MPO. The intensity SymHMin* of original moderate storms (> −100 nT) also increases up to −200 nT. These are important findings in

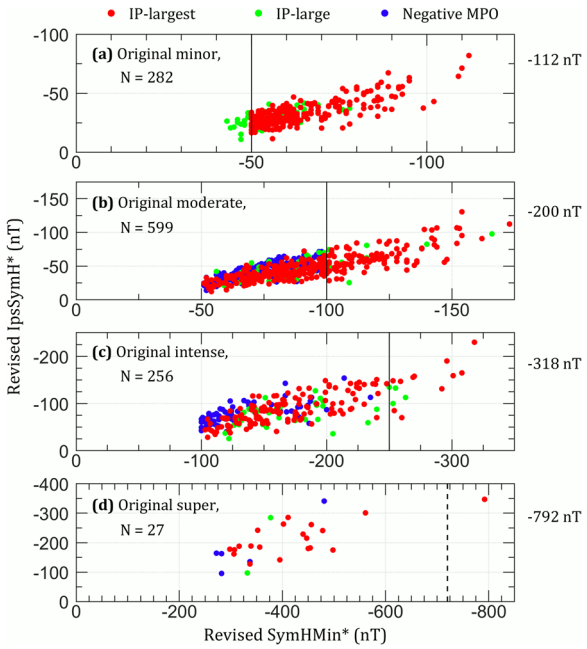

Fig. 4 Distribution of the revised storm intensity (X-axis) and revised impulsive strength (Y-axis) of the original 282 minor storms (**a**), 599 moderate storms (**b**), 256 intense storms and 27 super storms. The red and green dots indicate the storms having IP-largest and IP-large as positive MPO and blue dots indicate the storms having negative MPO. The vertical lines in **a**–**c** indicate the upper limits of minor, moderate and intense storms, and dashed line in (d) indicates the largest original SymHMin (− 720 nT)

understanding the high geo-effectiveness of the comparatively weak storms.

Identification of SvSW and MSW events

Definitions

The space weather events reported causing electric power outage and/or telecommunication system failure, which are of most concern to the public, are defined as severe space weather (SvSW) events (Balan et al. 2019a, 2024). Some other space weather events are reported causing minor system damages such as capacitor tripping in transformers, high voltage in power grids, etc. (e.g., Kappenman 2003). We define such space weather events as minor-system-damage space weather (MSW) events. The space weather events not causing such damaging effects are defined as normal space weather (NSW) events.

Table 3 lists the 3 severe space weather (SvSW) events and 8 minor-system-damage space weather (MSW) events reported since 1981. The SvSW events on 13 March 1989, 06 November 2001 and 30 October 2003, respectively, correspond to the power outage in Quebec (e.g., Medford et al. 1989; Boteler 2019), New Zealand (Marshall et al. 2013) and Sweden (Pulkkinen et al. 2005). The MSW events on 13 April 1981, 08 February 1986 and 24 March 1991 and 31 March 2001, respectively, correspond to the transformer problems in Canada (The Northern Engineer, 1981), high voltage in power grids in Sweden (Stauning 2013) and two capacitor tripping in transformers in the US (Kappenman 2003). The MSW events on 08 November 1991 and 29 October 2003 measured the largest GIP and GIC (geomagnetically induced potential and current) in Sweden (Lundstedt 2006; Pirjola and Boteler 2006), and the MSW events on 07–10 November 2004 and 15 May 2005, respectively, measured the largest GIC at mid and low latitudes and highest G-level in the NOAA Space Weather Scales though monitoring systems likely prevented technological damages (Trivedi et al. 2007; Liu et al. 2009).

Identification of events

Figure 5 compares the capability of the corrected (revised) storm impulsive strength IpsSymH* and the uncorrected (original) impulsive strength IpsSymH to

Table 3 List of the 3 SvSW events (top) and 8 MSW events (bottom) reported since 1981

Type of event	Date	Remarks	References
SvSW - M	13-Mar-1989	Power outage in Quebec	Medford et al. (1989)
SvSW - N	06-Nov-2001	Power outage in New Zealand	Marshall et al. (2013)
SvSW - O	30-Oct-2003	Power outage in Sweden	Pulkkinen et al. (2005)
MSW - 1	13-Apr-1981	Transformer problems in Canada	The Northern Engineer, 1981
MSW - 2	08-Feb-1986	High voltage in power grids in Sweden	Stauning (2013)
MSW - 3	24-Mar-1991	Capacitor tripping in transformers in the US	Kappenman (2003)
MSW - 4	08-Nov-1991	Largest GIP (~ 27 V) in Sweden	Lundstedt (2006)
MSW - 5	31-Mar-2001	Capacitor tripping in transformers in the US	Kappenman (2003)
MSW - 6	29-Oct-2003	Largest GIC > 100A in Finland	Lundstedt (2006)
MSW - 7	07-Nov-2004	Largest GIC at mid and low latitudes	Trivedi et al. (2007), Liu et al. (2009)
MSW - 8	15-May-2005	Highest G-level in NOAA SWS	Trichtchenko et al. (2007)

The letters M, N and O and numbers 1–8 (column 1) are used to indicate these events in Fig. 5. Columns 2–4 list the event date, damage/problem and reference

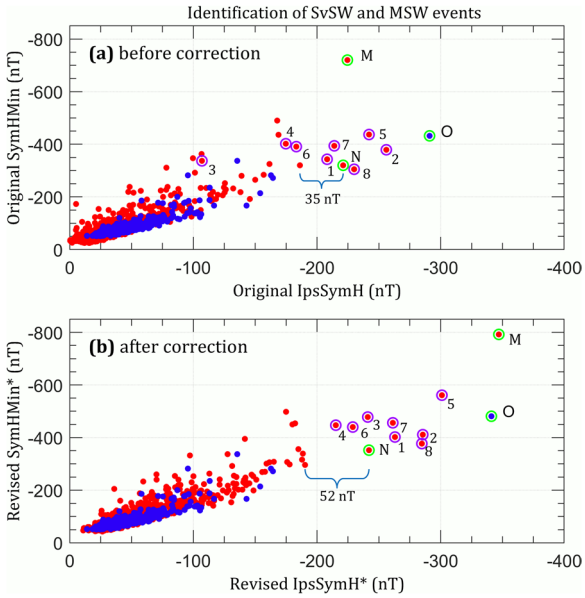

Fig. 5 Scatter plots of **a** original SymHMin against IpsSymH and **b** revised SymHMin* against IpsSymH* of the 1164 storms including 848 storms having positive MPO. Green circles and letters M, N and O indicate the 3 SvSW events and purple circles and numbers 1–8 indicate the 8 MSW events; blue and red dots alone indicate NSW events having positive and negative MPO

identify the severe space weather (SvSW) events and minor-system-damage space weather (MSW) events from normal space weather (NSW) events. The revised IpsSymH* identifies all 3 SvSW events (Fig. 5b, green circles and letters M, N and O) from all NSW events with a large separation of 52 nT compared to a separation of 35 nT by the original IpsSymH (Fig. 5a). The IpsSymH* also identifies all 8 MSW events (purple circles and numbers 1–8) though with a smaller separation, while original IpsSymH identifies only 5 MSW events. The revised and original storm intensity (Fig. 5, Y-axes), however, identifies only 1 SvSW event each. In Fig. 5, except for the one green circle noted by the letter O, all other green and purple circles have red dots inside indicating that all these storms have (large) positive MPO. The one SvSW event that has blue dot (indicating negative MPO) is the well-known Halloween event on 30 October 2003, which is the second of the super double storms during 29–31 October 2003. Though the second storm has negative MPO, the correction for the positive MPO of the first storm increased the IpsSymH* of the second storm as well indicating not only the power outage (Pulkkinen et al. 2005) but also the largest ever recorded positive ionospheric storm and fastest equatorward neutral wind (e.g., Mannuuci et al. 2005; Balan et al. 2011). The observations highlight that the correction for the positive MPO is most important for the storm impulsive strength

It may be noted that the reporting of space weather related technological problems is non-uniform and there were only very few reports from the Southern hemisphere, China and Russia. The power grid outages and communication failures could also be minimized over time due to technological improvements. Also, the lower ends of the revised IpsSymH* of SvSW and MSW events are approximately −240 nT and −210 nT (Fig. 5b). These observed values need not be thresholds. There might have been SvSW and MSW events for lower values of revised IpsSymH*, which might not have been reported.

Discussion

The main point of this paper is the correction for the missed important early part of MP from positive MPO to original 0-level. Here we briefly discuss the importance of solar wind dynamic pressure P and IMF Bz on the correction by considering a sample case (Fig. 6). As shown, the major decreasing part 2 (67%, 60 out of 90 nT) of the missed part of MP (panel a) occurs after IMF Bz turns southward (panel b). While only a minor decreasing part 1 (33%) occurs when the dynamic pressure P decreases (panel c), IMF Bz remains northward (panel b) and polar cap potential (PCP) is low (panel d). Figure 6 also indicates that the initial large sudden increase of IP is most probably due to the sudden compression of the magnetosphere at the impulsive impact of the ICME front of suddenly increased P and IMF Bz highly northward, and the following slowly increasing part of IP is most probably due to the eastward magnetopause current induced by the slowly increasing P when IMF Bz remains highly northward. Detailed studies including model calculations for the relative effects of P and IMF Bz (e.g., Burton el at. 1975b; Araki et al. 1997; Shue et al. 1998) for all 814 storms having positive MPO are needed to fully explain the physical meaning of the correction, which will be published as a follow up paper. Such a detailed study is beyond the scope of the present paper.

The correction for positive MPO is most important for the revised impulsive strength IpsSymH* because it seems to fully capture the important physical processes such as the impulsive impact of fast ICME shock/front, magnetopause compression, high energy input, etc. The corrected IpsSymH* clearly identifies all 3 severe space weather (SvSW) events from all normal space weather (NSW) events with a large separation of 52 nT compared to a separation of 35 nT by the uncorrected IpsSymH; IpsSymH* also identifies all 8 minor-system-damage space weather (MSW) events form NSW events. However, the conventionally used storm intensity (both original SymHMin and revised SymHMin*) identifies only 1 SvSW event each probably because the intensity being proportional only to the maximum energy input misses

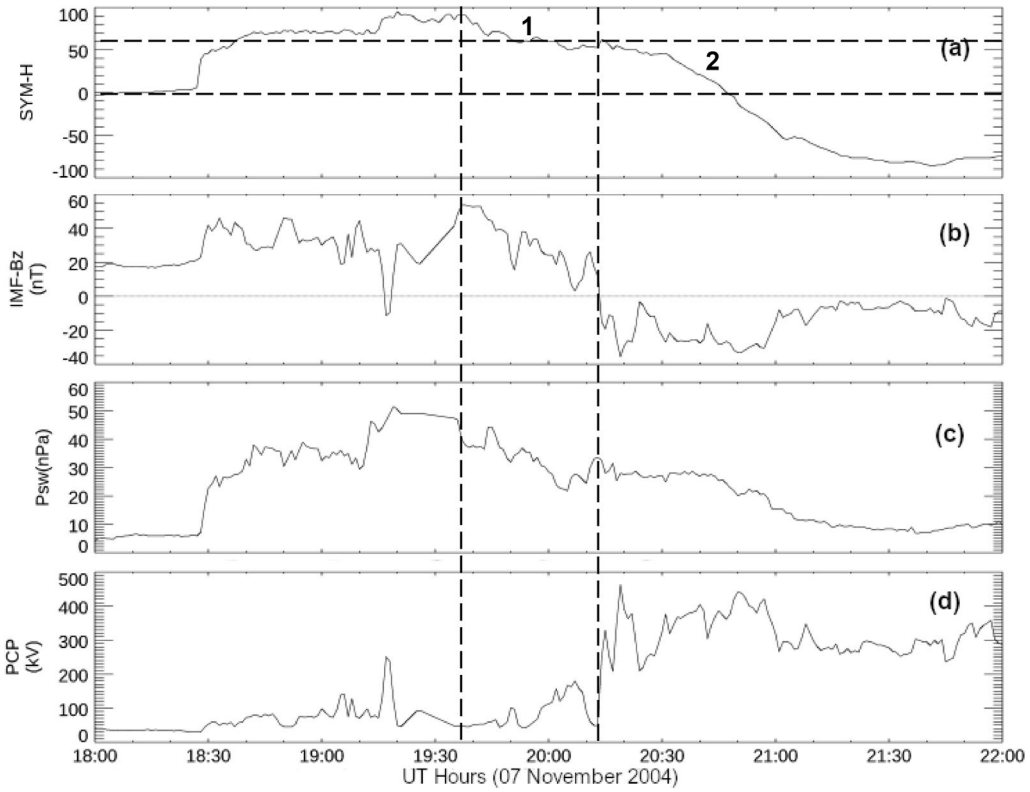

Fig. 6 Variations of SymH index (**a**), IMF Bz (**b**), solar wind dynamic pressure P (**c**) and polar cap potential PCP (**d**) during the positive initial phase IP of the geomagnetic storm on 07 November 2004. The vertical lines correspond to the main phase onset (MPO) in SymH and IMF Bz turning southward. The decreasing parts 1 and 2 of SymH before and after IMF Bz turns southward are noted

the impulsive action of ICME. However, the revised SymHMin* largely changes the conventional storm identification and classification. In addition, the revised IpsSymH* helps understand the high geo-effectiveness of the second storm of super double storms. In ionosphere-thermosphere studies, the correction may help understand how the comparatively weak and moderate geomagnetic storms especially under low solar activity correspond to extremely large ionosphere-thermosphere storms (e.g., Lei et al. 2018; Alphonsi et al. 2021; Rajesh et al. 2021) including the loss of Space-X satellites (e.g., Dang et al. 2022; Lookwood et al. 2023).

The mechanism of large impulsive strength IpsSymH* (high-energy input over a short duration) probably begins through continuous and rapid magnetic reconnection (e.g., Dungey 1961; Sonnerup 1984; Borovsky et al. 2008). This important physical process seems to happen when fast ICMEs with high front velocity ΔV (sudden increase by over 275 km s^{-1}) and sufficiently large IMF Bz southward at and beyond the velocity increase impacts the magnetopause (e.g., Balan et al. 2017b). The Bz southward opens the dayside magnetopause and high ΔV (and high V) provides the force for the impulsive entry of a large number of high-energy charged particles into the magnetosphere and ionosphere. The coherence of the global parameters high ΔV and large Bz southward leading to another global parameter (large IpsSymH*) and regional phenomena (SvSW and MSW) reveals an impulsive solar wind-magnetosphere-ionosphere-ground system coupling. The impulsive coupling results in an intense regional ionospheric current somewhere at high latitudes (e.g., Boteler 2019), which generates strong geomagnetic field fluctuations reaching down the Earth, which in turn induces strong secondary currents and voltages in the Earth (and Earth systems) of large electrical conductivity (Viljanen et al. 2010). These induced currents and voltages exceeding the tolerance limit of the vulnerable systems cause system failures (e.g., Albertson et al. 1974; Lanzerotti 1983; Kappanman 2003).

Conclusions

The correction for the missed important early decreasing part of the main phase (MP) from positive MPO to original 0-level of SymH accounts for the full range of MP of the geomagnetic storms. The corrected (revised) storm intensity (SymHMin*) increasing by up to −149 nT

changes the conventional storm identification and classification. The impulsive action of the ICME impact on the magnetosphere-ionosphere system happens during the corrected important early part of MP, which is fully reflected in the corrected impulsive strength IpsSymH* increasing by up to −134 nT. The corrected IpsSymH* clearly identifies all 3 reported severe space weather (SvSW) events causing electric power outage and/or telecommunication system failure from over 1100 normal space weather (NSW) events with a large separation of 52 nT compared to a separation of 35 nT by the uncorrected IpsSymH; IpsSymH* also identifies all 8 minor-system-damage space weather (MSW) events.

Acknowledgements
We thank Kyoto WDC (http://wdc.kugi.kyoto-u.ac.jp/aeasy/index.html) for the SymH data. N. Balan and Qing-He Zhang thank National Natural Science Foundation (Grants 42120104003, 41904169 and 41874170) and the Stable-Support Scientific Project of China Research Institute of Radio wave Propagation (Grant No. A132101W02) for supporting the study.

Author contributions
VM and NB initiated the study and prepared the paper. VM developed the computer program, did most of the data analysis and participated in the preparation of the paper. YB contributed in discussing the physical meaning of the correction. QHZ and ZYX are involved in the discussions. All authors read and approved the final manuscript.

Funding
This study is supported by the National Natural Science Foundation (Grants 42120104003, 41904169 and 41874170) and the Stable-Support Scientific Project of China Research Institute of Radio wave Propagation (Grant No. A132101W02).

Availability of data
The SymH index is downloaded from http://wdc.kugi.kyoto-u.ac.jp/aeasy/index.html and Solar Wind-IMF data is downloaded from https://omniweb.gsfc.nasa.gov/form/omni_min.html.

Declarations

Competing interests
The authors declare that they have no competing interests.

Author details
[1]Institute of Space Sciences, Shandong University, Weihai 264209, China. [2]Institute of Space Earth Environment Research, Nagoya University, Nagoya, Japan. [3]Research Institute for Sustainable Humanosphere, Kyoto University, Uji, Japan.

Received: 18 September 2023 Accepted: 4 April 2024
Published online: 29 April 2024

References

Akasofu SI (1981) Energy coupling between the solar wind and the magnetosphere. Space Sci Rev 28:121–190. https://doi.org/10.1007/BF00218810
Akasofu SI (2021) A review of studies of geomagnetic storms and auroral/magnetospheric substorms based on the electric current approach. Front Astron Space Sci 7:100
Albertson VD, Thorson JM, Miske SA (1974) The effects of geomagnetic storms on electrical power systems. IEEE Trans Power Appar Syst 4:1031–1044
Alfonsi L, Cesaroni C, Spogli L, Regi M, Paul A, Ray S et al (2021) Ionospheric disturbances over the Indian sector during 8 September 2017 geomagnetic storm: plasma structuring and propagation. Space Weather 19:e2020SW002607. https://doi.org/10.1029/2020SW002607
Araki T (2014) Historically largest geomagnetic sudden commencement (SC) since (1868). Earth Planets Space 66(1):1–6
Araki T et al (1997) Anomalous sudden commencement on March 24, 1991. J Geophys Res 102(A7):14075–14086. https://doi.org/10.1029/96JA03637
Balan N, Alleyne H, Walker S, Reme H, McCrea I, Aylward A (2008) Magnetosphere-ionosphere coupling during the CME events of 07–12 November 2004. J Atmos Solar Terr Phys. https://doi.org/10.1016/j.jastp.2008.03.015
Balan N, Yamamoto M, Liu JY, Otsuka Y, Liu H, Lühr H (2011) New aspects of thermospheric and ionospheric storms revealed by CHAMP. J Geophys Res 116:A07305. https://doi.org/10.1029/2010JA016399
Balan N, Otsuka Y, Nishioka M, Liu JY, Bailey G (2013) Physical mechanisms of the ionospheric storms at equatorial and higher latitudes during MP and RP of geomagnetic storms. J Geophys Res 118:2660. https://doi.org/10.1002/jgra.50275
Balan N, Batista IS, Tulasi Ram S, Rajesh PK (2016) A new parameter of geomagnetic storms for the severity of space weather. Geosci Lett 3(1):1–5
Balan N, Tulasiram S, Kamide Y, Batista IS, Souza JR, Shiokawa K et al (2017a) Automatic selection of Dst storms and their seasonal variations in two versions of Dst in 50 years. Earth Planets Space 69(1):59. https://doi.org/10.1186/s40623-017-0642-2
Balan N, Ebihara Y, Skoug R, Shiokawa K, Batista IS, Tulasi Ram S et al (2017b) A scheme for forecasting severe space weather. J Geophys Res Space Physics 122(3):2824–2835. https://doi.org/10.1002/2016JA023853
Balan N, Zhang QH, Xing Z, Skoug R, Shiokawa K, Lühr H, Ram T, Otsuka Y, Zhao L (2019a) Capability of geomagnetic storm parameters to identify severe space weather. Astrophys J 887(1):51
Balan N, Zhang Q-H, Shiokawa K, Skoug R, Xing Z, Tulasi Ram S, Otsuka Y (2019b) IpsDst of Dst storms applied to ionosphere-thermosphere storms and low latitude aurora. J Geophys Res 124:9552. https://doi.org/10.1029/2019JA027080
Balan N, Ram ST, Manu V, Zhao L, Xing Z, Zhang Q (2021) Diurnal UT variation of low latitude geomagnetic storms using six indices. J Geophys Res Space Physics 126(10):e2020JA028854. https://doi.org/10.1029/2020JA028854
Balan N, Zhang QH, Tulasi Ram S, Shiokawa K, Xing Z-Y (2024) How to identify and forecast severe space weather events. J Atmo Sol Terr Phys. https://doi.org/10.1016/j.jastp.2024.106183
Borovsky JE, Hesse M, Birn J, Kuznetsova MM (2008) What determines the reconnection rate at the dayside magnetosphere? J Geophys Res Space Phys. https://doi.org/10.1029/2007JA012645
Boteler DH (2019) A 21st century view of the March 1989 magnetic storm. Space Weather 17(10):1427–1441
Burton RK, McPherron RL, Russell CT (1975a) The terrestrial magnetosphere: A half-wave rectifier of the interplanetary electric field. Science 189(4204):717–718
Burton RK, McPherron RL, Russell CT (1975b) An empirical relationship between interplanetary conditions and Dst. J Geophys Res 80(31):4204–4214. https://doi.org/10.1029/ja080i031p04204
Chapman, S., & Bartels, J. (1940). Geomagnetism, Vol. II: Analysis of the data, and physical theories. London: Oxford University Press.
Daglis IA (1997) The role of magnetosphere-ionosphere coupling in magnetic storm dynamics. In: Tsurutani BT, Gonzalez WD, Kamide Y, Arballo JK Eds. Magnetic storms. Geophysical Monograph Series (Vol. 98, pp. 107–116). https://doi.org/10.1029/GM098p0107
Dang T, Li X, Luo B, Li R, Zhang B, Pham K et al (2022) Unveiling the space weather during the Starlink satellites destruction event on 4 February 2022. Space Weather 20:e20220SW03152. https://doi.org/10.1029/2022SW003152
Dungey JW (1961) Interplanetary magnetic field and the auroral zones. Phys Rev Lett 6(2):47
Ebihara Y, Ejiri M (2003) Numerical simulation of the ring current: *Review*. Space Sci Rev 105:377. https://doi.org/10.1023/A:1023905607888
Ebihara Y et al (2005) Ring current and the magnetosphere-ionosphere coupling during the super storm of 20 November 2003. J Geophys Res 110:A09S22. https://doi.org/10.1029/2004JA010924
Fuller-Rowell TJ, Codrescu MV, Moffett RJ, Quegan S (1994) Response of the thermosphere and ionosphere to geomagnetic storms. J Geophys Res Space Phys 99(A3):3893–3914

Gonzalez WD, Joselyn JA, Kamide Y, Kroehl HW, Rostoker G, Tsurutani BT, Vasyliunas VM (1994) What is a geomagnetic storm? J Geophys Res 99(A4):5771. https://doi.org/10.1029/93ja02867
Gonzalez WD, Echer E, Tsurutani BT, Clúa de Gonzalez AL, Dal Lago A (2011) Interplanetary origin of intense, super intense and extreme geomagnetic storms. Space Sci Rev 158(1):69–89. https://doi.org/10.1007/s11214-010-9715-2
Gopalswamy N, Yashiro S, Xie H, Akiyama S, Mäkelä P (2015) Properties and geoeffectiveness of magnetic clouds during solar cycles 23 and 24. J Geophys Res Space Phys 120(11):9221–9245. https://doi.org/10.1002/2015JA021446
Hutchinson JA, Wright DM, Milan SE (2011) Geomagnetic storms over the last solar cycle: a superposed epoch analysis. J Geophys Res 116(9):A09211. https://doi.org/10.1029/2011JA016463
Iyemori T, Araki T, Kamei T, & Takeda M (1992) Midlatitude geomagnetic indices ASY and SYM (provisional No. 1 1989). Kyoto University
Kappenman JG (2003) Storm sudden commencement events and the associated geomagnetically induced current risks to ground-based systems at low-latitude and midlatitude locations. Space Weather. https://doi.org/10.1029/2003SW000009
Lanzerotti LJ (1983) Geomagnetic induction effects in ground-based systems. Progress in Solar-Terrestrial Physics, pp.347–356.
Lei J, Huang F, Chen X, Zhong J, Ren D, Wang W et al (2018) Was magnetic storm the only driver of the long-duration enhancements of daytime total electron content in the Asian-Australian sector between 7 and 12 September 2017? J Geophys Res Space Phys 123:3217–3232. https://doi.org/10.1029/2017JA025166
Liu L, Liu C, Zhang B (2009) Effects of geomagnetic storm on UHV power grids in China. Power Syst Technol 33(11):1–5
Lockwood M, Owens MJ, Barnard LA (2023) Universal time variations in the magnetosphere and the effect of CME arrival time: analysis of the February 2022 event that led to the loss of Starlink satellites. J Geophys Res Space Phys 128:e2022JA031177. https://doi.org/10.1029/2022JA031177
Love JJ, Gannon JL (2009). Revised Dst and the epicycles of magnetic disturbance: 1958–2007 (Vol. 27). www.ann-geophys.net/27/3101/2009/
Luhr H, Xiong C, Olsen N, Le G (2017) Near-earth magnetic field effects of large-scale magnetospheric currents. Space Sci Rev 206(1–4):521–545. https://doi.org/10.1007/s11214-016-0267-y
Lundstedt H (2006) The sun, space weather and GIC effects in Sweden. Adv Space Res 37(6):1182–1191. https://doi.org/10.1016/j.asr.2005.10.023
Mannucci AJ, Tsurutani BT, Iijima BA, Komjathy A, Saito A, Gonzalez WD, Guarnieri FL, Kozyra JU, Skoug R (2005) Dayside global ionospheric response to the major interplanetary events of October 29–30, 2003 "Halloween Storms." Geophys Res Lett. https://doi.org/10.1029/2004GL021467
Manu V, Balan N, Zhang Q-H, Xing Z-Y (2022) Association of the main phase of the geomagnetic storms in solar cycles 23 and 24 with corresponding solar wind-IMF parameters. J Geophys Res Space Phys 127:e20220JA30747. https://doi.org/10.1029/2022JA030747
Manu V, Balan N, Zhang Q-H, Xing Z-Y (2023) Double superposed epoch analysis of geomagnetic storms and corresponding solar wind and IMF in solar cycles 23 and 24. Space Weather 21:e2022SW003314. https://doi.org/10.1029/2022SW003314
Marshall RA et al (2013) Observations of geomagnetically induced currents in the Australian power network. Space Weather 11:6–16. https://doi.org/10.1029/2012SW000849
Medford et al (1989) Transatlantic earth potential variations during the March 1989 magnetic storms. Geophys Res Lett 16(10):1145
Pirjola RJ, Boteler DH (2006) Geomagnetically Induced Currents in European High-Voltage Power Systems, 2006 Canadian Conference on Electrical and Computer Engineering, Ottawa, ON, Canada, 2006, pp. 1263–1266. https://doi.org/10.1109/CCECE.2006.277540.
Proless GW (1995) Ionospheric F region storms. In: Volland H (ed) Handbook of atmospheric electrodynamics. CRC Press, Boca Raton, pp 195–248
Pulkkinen A, Lindahl S, Viljanen A, Pirjola R (2005) Geomagnetic storm of 29–31 October 2003: geomagnetically induced currents and their relation to problems in the Swedish high-voltage power transmission system. Space Weather 3:S08C03. https://doi.org/10.1029/2004SW000123
Rajesh PK, Lin CH, Lin CY, Chen CH, Liu JY, Matsuo T et al (2021) Extreme positive ionosphere storm triggered by a minor magnetic storm in deep solar minimum revealed by FORMOSAT-7/COSMIC-2 and GNSS observations. J Geophys Res Space Phys 126:e2020JA028261. https://doi.org/10.1029/2020JA028261
Russell CT, McPherron RL (1973) Semiannual variation of geomagnetic activity. J Geophys Res 78(1):92–108. https://doi.org/10.1029/ja078i001p00092
Russell CT, McPherron RL, Burton RK (1974) On the cause of geomagnetic storms. J Geophys Res 79(7):1105–1109
Shue J-H, Song P, Russell CT, Steinberg JT, Chao JK, Zastenker G, Vaisberg OL, Kokubun S, Singer HJ, Detman TR, Kawano H (1998) Magnetopause location under extreme solar wind condition. J GeoPhys Res 3:17691–17770. https://doi.org/10.1029/98JA01103
Sonnerup BÖ (1984) Magnetic field reconnection at the magnetopause: an overview. Magn Reconnect Space Lab Plasmas 30:92–103
Stauning P (2013) Power grid disturbances and polar cap index during geomagnetic storms. J. Space Weather Space Clim. 3:e22. https://doi.org/10.1051/swsc/2013044
Sugiura M (1964) Hourly values of equatorial Dst for the IGY. Ann Int Geophys Year 35:9–45
Trichtchenko L, Zhukov A, Van der Linden R, Stankov SM, Jakowski N, Stanisławska I, Juchnikowski G, Wilkinson P, Patterson G, Thomson AWP (2007) November 2004 space weather events: real-time observations and forecasts. Space Weather. https://doi.org/10.1029/2006SW000281
Trivedi NB et al (2007) Geomagnetically induced currents in an electric power transmission system at low latitudes in Brazil: a case study. Space Weather 5:S04004. https://doi.org/10.1029/2006SW000282
Tulasi Ram S, Liu CH, Su SY (2010) Periodic solar wind forcing due to recurrent coronal holes during 1996–2009 and its impact on Earth's geomagnetic and ionospheric properties during the extreme solar minimum. J Geophys Res Space Phys. https://doi.org/10.1029/2010JA015800
Viljanen A, Koistinen A, Pajunpää K, Pirjola R, Posio P, Pulkkinen A (2010) Recordings of geomagnetically induced currents in the Finnish natural gas pipeline–Summary of an 11-year Period. Geophysica 46(1–2):59–67
Wang J, Guo Z, Ge YS, Du A, Huang C, Qin P (2018) The responses of the earth's magnetopause and bow shock to the IMF Bz and the solar wind dynamic pressure: a parametric study using the AMR-CESE-MHD model. J Space Weather Space Clim. 8:A41
Yermolaev YI, Lodkina IG, Khokhlachev AA, Yermolaev MY, Riazantseva MO, Rakhmanova LS et al (2021) Drop of solar wind at the end of the 20th century. J Geophys Res Space Phys 126:e2021JA029618. https://doi.org/10.1029/2021JA029618
Zong QG, Yue C, Fu SY (2021) Shock induced strong substorms and super substorms: preconditions and associated oxygen ion dynamics. Space Sci Rev 217(2):1–34

Publisher's Note